View metadata, citation and similar papers at core.ac.uk

brought to you by CORE

30-nm Scale Fabrication of Magnetic Tunnel Junctions Using EB Assisted CVD Hard Masks

Shinji Isogami[1], Masakiyo Tsunoda[1], and Migaku Takahashi[1,2]

[1]Department of Electronic Engineering, Tohoku University, Sendai 980-8579, Japan

[2]New Industry Creation Hatchery Center, Tohoku University, Sendai 980-8579, Japan

30-nm scale fabrication of magnetic tunnel junctions (MTJs) was demonstrated. A scanning electron microscope (SEM) was used for chemical–vapor deposition (CVD) of carbon hard masks. Using electron beam (EB)-CVD, less than several 10-nm scale carbon pillar could be formed on MTJ films. Argon ion milling, of which incident angle from the normal of the film plane was determined 45° and 75°, was utilized to pattern the MTJs. TMR properties of 80-nm scale MTJs were successfully measured using DC-four-probe at room temperature.

***Index Terms*—Argon ion milling, chemical–vapor deposition (CVD), magnetic tunnel junctions (MTJs), scanning-electron microscope (SEM).**

I. Introduction

In order to achieve ultrahigh areal recording density of hard disk drives (HDDs) and magnetic random access memories (MRAMs), downsizing of the magnetoresistive elements is indispensable. For instance, in case of spin valve elements in HDDs using current-perpendicular-to-plane (CPP) geometry, it is estimated that the elements should be several 10 nm width or less for over 500 Gbpsi [1]. In recent nano-fabrication process, electron-beam (EB) lithography or focused ion beam (FIB) etching are usually used in order to form a mask for Ar ion milling or direct patterning of the elements. However, their achievable element width is $\sim$80 nm in general. This is because, the organic-resist is easy to make the deformation during Ar ion milling for EB lithography, and an injection of Ga ion dysfunctions the edge part of elements about 5 nm thick for FIB patterning. In order to overcome these problems, FIB-assisted chemical–vapor deposition (CVD) hard mask method is developed [2], [3]. However, it still has a problem of Ga injection into the top of elements about 30 nm depth. In this study, we demonstrated EB-assisted CVD carbon hard mask method, instead of FIB. Deposited carbon pillar could be used as a mask for Ar ion milling and also a via contact to top electrode in the final nano-scaled devices. We succeeded in the carbon pillar deposition with minimum size of 30 nm width under the well optimized condition. After CVD of carbon pillar, we demonstrated the patterning of the MTJ films. Tuning the angles of Ar ion milling and O_2 ion ashing in the best etching angle, MTJ films were well patterned with the same width of the mask.

II. Experimental Procedure

A. Film Preparation and Measurement of MTJs

MTJ films, Sub./Ta(5)/Cu-O(40)/Ta(5)/NiFe(2)/Cu(5)/$Mn_{75}Ir_{25}$(10)/$Co_{70}Fe_{30}$(4)/Al-Nitride(1)/$Co_{70}Fe_{30}$(4)/NiFe(20)/Ta(5), were prepared by DC magnetron sputtering on Si(100) substrate with thermally oxidized layer. Number in parenthesis is the thickness of each layer in nm-unit. The barrier formation was performed by depositing metal Al film and subsequent nitriding it in the chamber with a radial line microwave antenna (RLSA) [4], [5]. Base pressure of the sputtering chamber was 9×10^{-9} Torr. TMR measurement was carried out using DC-four-probe method at room temperature. Applied field was varied from -0.3 kOe to $+0.3$ kOe.

B. Deposition of Carbon Pillar Using EB-CVD

Fig. 1 shows the fabrication process of nano-scaled MTJs. Dual-beam FIB equipment, DB235M (FEI Co.) was used for deposition and observation of carbon pillar [in Fig. 1(a)]. Electron beam was generated at field emission type filament, and its extractor voltage was fixed 5 kV. EB was accelerated by various voltages of 1–30 kV. The probe current was measured using a Faraday cup. The probe diameter was approximately less than 5 nm in 30 kV. The gas source was phenanthrene ($C_{14}H_{16}$) powder in the gas injection source (GIS) column. The source was heated up to 303 K and kept opening the GIS column shutter during deposition to fill up the vacuum chamber with the injected gas of 2×10^{-4} Pa. $C_{14}H_{16}$ was decomposed on the surface of the MTJ film into solid of carbon due to EB energy. Height and width of piled up pillars were measured using SEM observation.

C. ECR Etching for Patterning

Electron cyclotron resonance (ECR) ion beam shower system, EIS-200ER (ERIONIX Co.), was used for patterning the MTJ films in nano-scale junctions. Microwave power was fixed at 100 W. Ar (O_2) ion was accelerated by a voltage of 300 V (250 V) and emission current was 0.6 mA/cm^2 (0.45 mA/cm^2), respectively. Both of etching gas pressure were 0.009 Pa. Etching depth from the surface of MTJ film was 30 nm. Ar ion milling process was divided into two stages according to the etching angle; 45° for first stage [Fig. 1(b1)] and 75° for second stage [Fig. 1(b2)], where etching angle was measured from the normal of the film plane. In first stage, MTJs were milled into vertical direction mainly. Next in second stage, side

Digital Object Identifier 10.1109/TMAG.2005.854786

0018-9464/$20.00 © 2005 IEEE

Authorized licensed use limited to: TOHOKU UNIVERSITY. Downloaded on October 28, 2008 at 22:47 from IEEE Xplore. Restrictions apply.

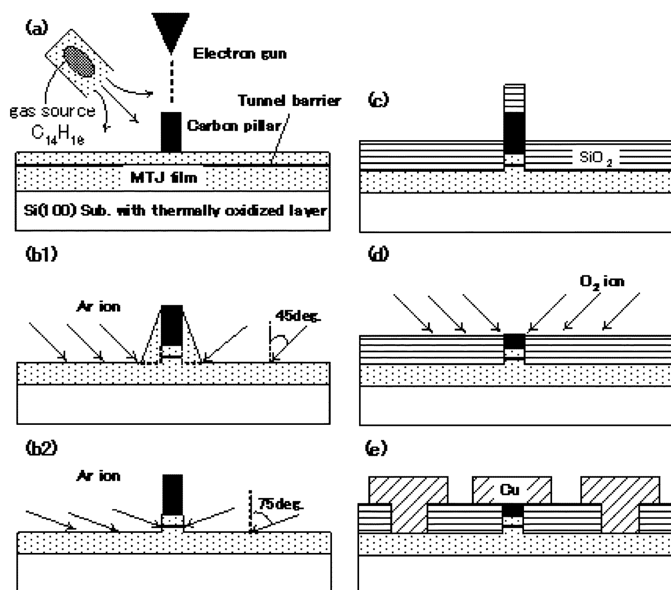

Fig. 1. Schematic diagram of fabrication process. (a) Deposition of carbon pillar using EB exposure on MTJ film. (b1) Patterning of MTJs by Ar ion milling in 45°. (b2) Patterning of MTJs by Ar ion milling in 75°. (c) Deposition of SiO_2. (d) O_2 ashing for lowering the pillar height. (e) Nano-fabricated device.

wall which was re-deposited layer from the MTJ film was able to be removed. They were the optimized angle condition of all trial in this study. O_2 ashing process was applied after the Ar ion milling [in Fig. 1(d)]. The etching angle was determined 45° and etching time was 60 s. Before and after O_2 etching, specimens were observed using SEM.

III. Results and Discussion

A. Deposition Performance

Since the performance of carbon pillar deposition depends on the EB acceleration voltage and probe diameter mainly, it is necessary to investigate the correlation with probe current. Fig. 2 shows the acceleration voltage and probe size dependence of EB probe current. As the acceleration voltage and probe size became larger, probe current was also increased nonlinearly.

In Fig. 3, we can see that very thin needle like pillar with 30 nm width is piled up with 90° of taper-angle to the MTJ film plane. Because of the much smaller mass of electron than that of ion and resultant mild kinetic energy of EB to deposite the minute and stable pillar, the amount of carbon deposited around the foot of pillar (so called "tail") is much less than the FIB case [2]. From practical point of view, no tailed pillar is necessary for elements to be patterned as the same width as the mask because the tail also works as the etching mask.

Fig. 4 shows the probe current dependence of deposited pillar width and height. In order to deposite the pillar as small width as possible, probe current was varied from 4 to 16 pA. In case that the probe current was lower than 4 pA, pillar shape tended to be low height and wide width. As the probe current was higher, pillar height could increase and width could decrease, simultaneously. The decreasing width might be due to the improved EB current stability, such as fluctuation of current and probe spot position, resulting in the well focused EB energy on the film surface. In the case that probe current was more than 15 pA, height

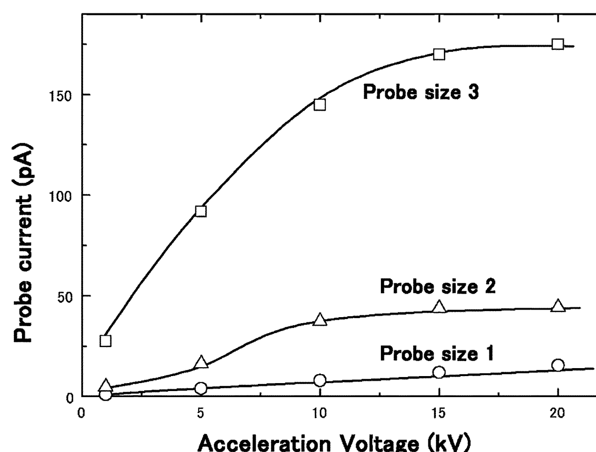

Fig. 2. Acceleration voltage and probe size dependence of probe current. The probe size1 (open circle) was smallest spot, less than 5 nm.

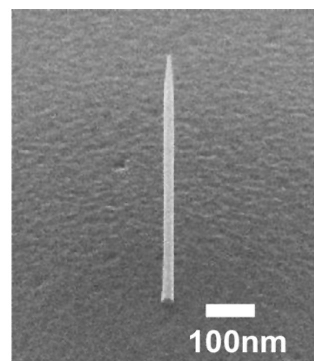

Fig. 3. SEM image of carbon pillar deposited on a TMR film using EB-assisted CVD whose probe current was 14 pA. Its size was 30 nm width and 1300 nm height.

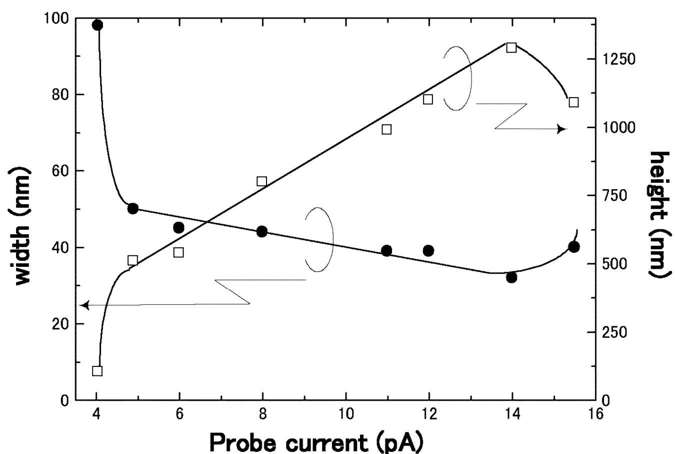

Fig. 4. Probe current dependence of deposited pillar width (closed circle) and height (open square). Deposition time was 3 min.

decreased and width increased. This effect could be elucidated as follows. EB energy came to be large, decomposition rate of phenanthrene was generally promoted. However in case that the EB energy was too large, evaporation effect of carbon came to dominate compared with deposition on to the head of pillar. Moreover, since diffusion effect of decomposed solid carbon became also large, the pillar width tended to be wide. Therefore, we found that probe current of 14 pA was the best EB condition

Authorized licensed use limited to: TOHOKU UNIVERSITY. Downloaded on October 28, 2008 at 22:47 from IEEE Xplore. Restrictions apply.

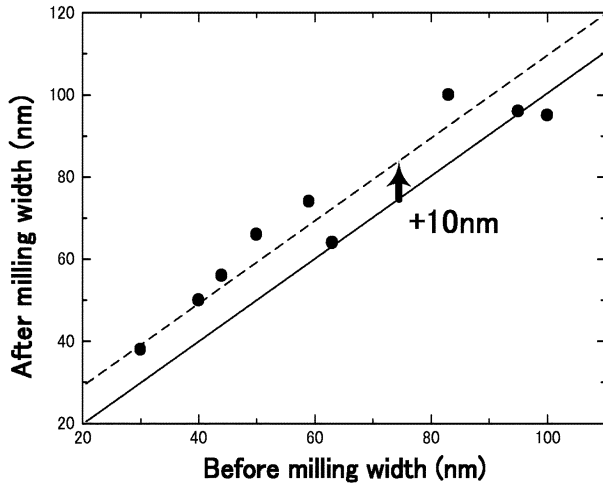

Fig. 5. Comparison of the element width between before and after Ar ion milling. Solid and dashed lines indicate after = before case and after = before+ 10 nm case, respectively. Milling angles were 45°, 75° (filled circle).

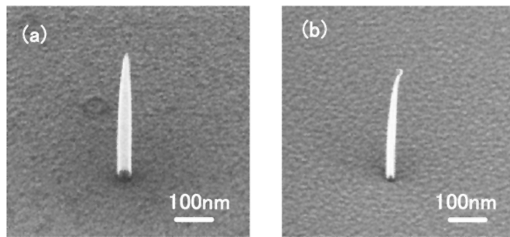

Fig. 6. SEM images of carbon pillar piled up on the TMR surface. (a) and (b) indicates the pillar with and without O2 ion ashing, respectively. The (height, width) of pillar was (970 nm, 62 nm) for (1) and (840 nm, 38 nm) for (2). The O_2 ion ashing was applied for 60 s in 45°.

for piling up the smallest pillar which had 30 nm width (Fig. 4) under the present experimented conditions.

B. ECR Etching

ECR ion beam were showered on the MTJ film surface with carbon mask for patterning it in nano-scaled MTJs. Fig. 5 shows the comparison of the element width between before and after Ar ion milling. We can see that after-milling element width could have a +10 nm biased linear relation with before one. However, a few elements, such as 63, 95, and 100 nm of before milling width for example, could be patterned without width-change at the after state. Though the reason why there is a difference relation between these a few elements and the other elements is not elucidated at the present, we have a possibility to obtain MTJs with the same width as the mask one even though its width is very small.

Since resistance of whole MTJs will be large when we use a tall carbon pillar as via contact electrode, the pillar height should be decreased down to SiO_2 level by O_2 ion ashing in actual fabrication process [Fig. 1(d)]. Fig. 6 shows 52° tilted SEM images of carbon pillar at before and after O_2 ion ashing in 60 s. The volume of carbon pillar was decreased by 68% selectively. However, another material of Ta plane on which the carbon pillar piled up was not so changed according to the contrast change between Fig. 6(a) and (b). This is because that the carbon (Ta) showed a very high (low) etching rate for O_2. We thus say that applying the O_2 ashing to the carbon pillar, decreasing the pillar height was possible without any damages for MTJ film surface.

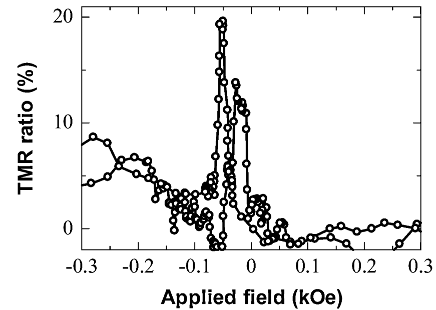

Fig. 7. TMR measurement of MTJ with 80 nm width at room temperature.

C. TMR Measurement Using DC-Four-Probe Method

Fig. 7 shows the result of TMR measurement of MTJ with 80 nm width at room temperature. While TMR curve was not stable due to thermal noise, TMR ratio of approximately 20% was observed. The resistance of this nano-fabricated MTJ was 10 MΩ and its calculated *RA* value with an area of 80 nm width came to be 10^5 $\Omega\mu$m^2. This *RA* value is comparable to that of the TMR film used in the present study, 5×10^5 $\Omega\mu$m^2 [4].

Since the present fabrication of barrier layer employs only the physical etching by Ar ion and is independent of any chemical reactive process, it can be applicable to the MTJs with other barrier layer materials than Al-nitride.

IV. Summary

30-nm scale fabrication of MTJs using EB-assisted CVD of carbon mask was demonstrated. In this study, the minimum width of 30-nm carbon pillar was piled up at probe current of 14 pA. Carbon mask is hard for Ar ion milling and soft for O_2 ion ashing. Therefore, applying Ar ion milling with its angle of 45° and 75°, MTJs can be able to have the same width as the carbon mask. Moreover, applying O_2 ion ashing, smaller electrode was possible to achieve for lowering resistances of MTJs. Comparable TMR properties of nano-scale-fabricated MTJs were obtained. Using these fabrication processes, CPP-TMR/GMR element with 30 nm width can have the great potential for ultrahigh areal density of 500 Gbpsi.

References

[1] M. Takagishi, K. Koi, M. Yoshikawa, T. Funayama, H. Iwasaki, and M. Sahashi, *IEEE. Trans. Magn.*, vol. 38, pp. 2277–2282, Sep. 2002.
[2] H. Kubota, M. Hamada, Y. Ando, and T. Miyazaki, *J. Appl. Phys.*, vol. 93, p. 8370, 2003.
[3] D. Watanabe, H. Kubota, Y. Ando, and T. Miyazaki, *J. Magn. Soc. Jpn.*, vol. 28, p. 569, 2004.
[4] S. Yoshimura, T. Shoyama, T. Nozawa, M. Tsunoda, and M. Takahashi, *IEEE Trans. Magn.*, vol. 40, pp. 2290–2292, 2004.
[5] K. Nishikawa, M. Tsunoda, S. Ogata, and M. Takahashi, *IEEE Trans. Magn.*, vol. 38, pp. 2718–2720, Sep. 2002.

Manuscript received February 7, 2005.

Authorized licensed use limited to: TOHOKU UNIVERSITY. Downloaded on October 28, 2008 at 22:47 from IEEE Xplore. Restrictions apply.